MECSOL 2022 - Proceedings of the 8th International Symposium on Solid Mechanics
M.L. Bittencourt, J. Labaki, L.C.M. Vieira Jr. and E. Mesquita (Editors), Campinas SP, Brazil, October 17th to 19th, 2022

Displacement response of a 3D full-space due to time-harmonic, biquadratic loads

Edivaldo Romanini[1], Josué Labaki[2], Iago Cavalcante[2] and Euclides Mesquita[2]

[1] Federal University of South Mato Grosso, Tres Lagoas MS Brazil
[2] School of Mechanical Engineering, University of Campinas, Campinas SP Brazil

Abstract. This article presents solutions for the displacement fields of full-spaces subjected to external vertical loads. In this problem, the full-space is a three-dimensional, viscoelastic, isotropic, unbounded medium. The solution method consists of writing the coupled Navier-Cauchy differential equations describing the medium in terms of independent vector fields, in the sense of a Helmholtz decomposition. A subsequent Fourier transformation enables boundary conditions corresponding to the external loads to be incorporated algebraically. In this paper, the external loads are time-harmonic and have a biquadratic distribution over a rectangular area of the full-space. Expressions for these loads in the Fourier domain are derived and presented. Since closed-form, non-singular, analytical expressions were able to be obtained for these loads, the final displacement solutions can be used in the context of boundary element and meshless methods without the issue of singularities resulting from collocation, which is a major application of these solutions. In addition to this advantage, the fact that the solutions consider biquadratic loads enables an improved representation of sharply-varying contact traction fields, which are common in many engineering applications. Final expressions for displacement fields are presented in terms of double Fourier integrals. The paper discusses strategies for their accurate numerical evaluation, and presents selected numerical results.
Keywords: boundary element method, Green's functions, influence functions, quadratic elements

INTRODUCTION

The boundary element method (BEM) is typically the method of choice to model the soil and other unbounded media. The main reason for this is its ability to comply with the radiation condition of unbounded media (Sommerfeld, 1949) and because the BEM does not require truncation of the mesh in the domain (Kuzuoglu and Mittra, 1997).

One of the formulations of the BEM is the Direct-BEM (DBEM), in which a discretized boundary integral equation relates stress and displacement Green's functions for the medium being analyzed. Pan (2019) brings a somewhat updated, comprehensive literature review of Green's functions that have been derived for elasticity analyses using the DBEM. Formulations of the DBEM are known for their problems with singularities, which result from the collocation of singular Green's functions at the boundary of the problem (Dumont, 1994).

The Indirect formulation of the BEM (IBEM) proposes to sort this problem by using non-singular influence functions. In these functions, singularities resulting from coinciding source and field points are integrated analytically, so that the final displacement and stress fields are free from singularities, even if external loads are collocated directly at the boundary. In the IBEM, stress and displacement states are related through sets of unknown, fictitious loads, rather than directly through a boundary integral equation. These fictitious loads are then found by imposing that the displacement and stress states belong to the same problem. Some applications of non-singular influence functions in the context of the IBEM can be seen in Carneiro et al. (2022) for the problem of a surface wall and in Guerra et al. (2022) for the problem of large-diameter shafts.

The authors of this paper have invested the past decades deriving non-singular influence functions for various types of media, for their applications in DBEM and IBEM schemes. Among the successful results are influence functions for isotropic (Mesquita et al., 2012) and anisotropic media (Barros and Mesquita, 1999), harmonic and transient excitations (Mesquita et al., 2003), concentrated (Mesquita et al., 2009) and distributed loads, for half-spaces (Mesquita et al., 2012) and full-spaces (Labaki et al., 2019). A variety of different methods of derivation were investigated (Adolph et al., 2007; Romanini et al., 2019). The group has also invested in methods for the accurate numerical evaluation of these solutions (Labaki et al., 2012) and in advanced schemes to address their associated computational cost problem (Mesquita et al., 2009).

A variety of other influence functions are also available in the literature, which aim at representing other soil features, such as its transverse isotropy, poroelasticity, and the layered constitution commonly found in engineering practice. Fu et

al. (2017) and Fu et al. (2019) used these functions in an IBEM context to model the dynamic response of rectangular plates embedded in layered, transversely isotropic soils. Ba et al. (2018a) used this formulation to obtain the response of strip foundations in transversely isotropic, layered, elastic soils, which was later extended by Ba et al. (2018b) to the poroelastic case. The more arbitrarily-shaped problem of alluvial basins has been more recently addressed by Ba et al. (2020).

The motivation for the present paper is the case of discontinuous contact problems. These problems are common in systems involving more than one medium or more than one interacting body. The difficulty is that contact tractions at the interface between multiple media and bodies present sharp variation at their interfacing edge (Barros and Mesquita, 2000). These are difficult to represent accurately with influence functions that consider uniformly-distributed loadings, such as those derived by Romanini et al. (2019). In order to represent these tractions accurately with uniformly-distributed loading solutions, large number of elements are necessary, which aggravates the problem of the already high computational cost of these functions. Additionally, depending on the type of singularity experienced by these contact tractions, their representation may only be possible by influence functions that match their type of singularity exactly (Barros and Mesquita, 2009). Romanini et al. (2021) have recently put forward novel influence functions that consider external loads with bilinear variation, which is a significantly improvement towards representing these sharply-varying contact quantities. The solutions in the present article are yet another significant step towards solving this problem.

This article presents displacement solutions for a 3D, isotropic full-space under time-harmonic vertical loads. The solutions can consider the loads to have arbitrary biquadratic distribution over a rectangular area of the full-space. These influence functions can be thought of as quadratic boundary elements, which can be used in DBEM and IBEM frameworks and meshless methods to solve elastodynamic problems.

PROBLEM DEFINITION

Consider a 3D, isotropic full-space, subjected to time-harmonic loads of circular frequency ω applied in the vertical (z) direction. The loaded surface is a square patch defined by $|x| < A; |y| < B; z = 0$. The spatial distribution of the load over this area is considered to have arbitrary biquadratic variations (Fig. 1).

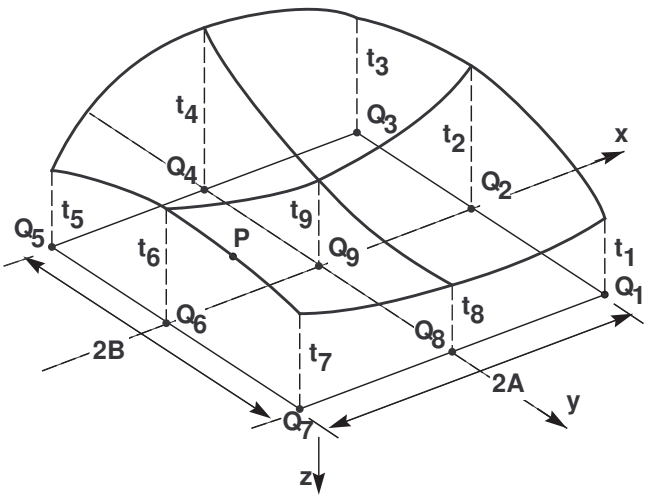

Figure 1 – Biquadratically-varying load distribution within the full-space.

It is a reasonable hypothesis for this problem to disregard body forces, without which the equation of motion for the full-space is given by

$$\mu\nabla^2 U + (\lambda+\mu)\nabla(\nabla \bullet U) = -\omega^2 \rho U. \tag{1}$$

In Eq. 1, μ and λ are Lamé's constants and ρ is the mass density of the full-space, and $U = U(x,y,z)$ is the displacement vector of an arbitrary point of coordinates (x,y,z). The corresponding stress field $\sigma = \sigma(x,y,z)$ can be obtained from U through the generalized Hooke's Law for the isotropic medium:

$$\sigma_{ij} = \lambda(\nabla \bullet U)\delta_{ij} + \mu(U_{i,j} + U_{j,i}), \tag{2}$$

in which δ_{ij} is the Krönecker Delta.

The problem to be solved in this paper consists of finding solutions for the displacement field U for the loading case illustrated in Fig. 1.

SOLUTION PROCEDURE

In this paper, a Helmholtz decomposition scheme is used to find an expression for the coupled displacement field in Eq. 1 (Helmholtz, 1858). According to this scheme, the terms u_i of U, $U = u_i\hat{e}_i$ $(i = x,y,z)$ are expressed as the linear superposition of two independent vector fields Δ and Ω:

$$u_i = -\frac{1}{k_L^2}\Delta_{,i} + \frac{2}{k_S^2}\mathrm{e}_{imn}\Omega_{n,m}, \tag{3}$$

in which k_L and k_S are primary and secondary wave numbers of the full-space, given by

$$k_L^2 = \frac{\omega^2\rho}{\lambda+2\mu} \tag{4}$$

and

$$k_S^2 = \frac{\omega^2\rho}{\mu}. \tag{5}$$

Analogously to the decomposition of u_i in terms of Δ and Ω, stress components σ_{ij} from Eq. 2 can also be decomposed in terms of Δ and Ω as

$$\frac{\sigma_{ij}}{\mu} = \delta_{ij}\frac{1-2n^2}{n^2}\Delta - \frac{2}{k_L^2}\Delta_{,ij} + \frac{2}{k_S^2}\left(\mathrm{e}_{ikl}\Omega_{l,kj} + \mathrm{e}_{jkl}\Omega_{k,li}\right), \tag{6}$$

in which $n^2 = k_L^2/k_S^2$. The problem of finding U is now reframed as the problem of finding Δ and Ω. Ansatz solutions for Δ and Ω can be proposed in the wave number domain (β,γ) as

$$\Delta^{(1,2)} = A^{(1,2)}k_L^2\mathrm{e}^{\pm\alpha_L z+\mathrm{i}(\beta x+\gamma y)}, \tag{7}$$

and

$$\Omega_j^{(1,2)} = B_j^{(1,2)}k_S^2\mathrm{e}^{\pm\alpha_S z+\mathrm{i}(\beta x+\gamma y)}. \tag{8}$$

The exponential terms in these trial solutions are planned so that Δ and Ω vanish for $x \to \pm\infty$, in order for them to satisfy the radiation condition (Sommerfeld, 1949). In Eqs. 7 and 8, the index m denote the two halves of the full-space: $m = 1$ refers to $(-\infty < z \leq 0)$, and $m = 2$ refers to $(0 \leq z < +\infty)$.

A property of the vector fields Δ and Ω is that they are curl-free and divergence-free, respectively. Mathematically, these properties can be expressed as

$$\mathrm{e}_{ijk}\Delta_{k,j} = 0 \tag{9}$$

and

$$\frac{\partial}{\partial x_i}\left[\mathrm{e}_{imn}\Omega_{n,m}\right] = 0. \tag{10}$$

Substituting Eqs. 9 and 10 into Eqs. 7 and 8 results in

$$\alpha_{L,S}^2 = \left(\beta^2+\gamma^2\right) - k_{L,S}^2, \tag{11}$$

and

$$B_3^{(1,2)} = \frac{\mp\mathrm{i}}{\alpha_S}\left(\beta B_1 + \gamma B_2\right). \tag{12}$$

Substituting Eqs. 7 and 8 into Eqs. 3 and 6 results in expressions for the displacement and stress components in the wave number domain:

$$u_X^{(1,2)} = \left\{ -A^{(1,2)} \mathrm{i}\beta \mathrm{e}^{\pm\alpha_L z} \pm \frac{2}{\alpha_S} \left[B_1^{(1,2)} \beta\gamma + B_2^{(1,2)} \left(\gamma^2 - \alpha_S^2\right) \right] \mathrm{e}^{\pm\alpha_S z} \right\} \mathrm{e}^{\mathrm{i}(\beta x + \gamma y)} \tag{13}$$

$$u_Y^{(1,2)} = \left\{ -A^{(1,2)} \mathrm{i}\gamma \mathrm{e}^{\pm\alpha_L z} \pm \frac{2}{\alpha_S} \left[B_1^{(1,2)} \left(-\beta^2 + \alpha_S^2\right) - B_2^{(1,2)} \beta\gamma \right] \mathrm{e}^{\pm\alpha_S z} \right\} \mathrm{e}^{\mathrm{i}(\beta x + \gamma y)} \tag{14}$$

$$u_Z^{(1,2)} = \left\{ \mp A^{(1,2)} \alpha_L \mathrm{e}^{\pm\alpha_L z} - 2\mathrm{i} \left[B_1^{(1,2)} \gamma - B_2^{(1,2)} \beta \right] \mathrm{e}^{\pm\alpha_S z} \right\} \mathrm{e}^{\mathrm{i}(\beta x + \gamma y)} \tag{15}$$

$$\sigma_{XX}^{(1,2)} = \mu \left\{ A^{(1,2)} \left(\beta^2 - \gamma^2 - \alpha_S^2 + 2\alpha_L^2\right) \mathrm{e}^{\pm\alpha_L z} \pm \frac{4\mathrm{i}\beta}{\alpha_S} \left[B_1^{(1,2)} \beta\gamma + B_2^{(1,2)} \left(\gamma^2 - \alpha_S^2\right) \right] \mathrm{e}^{\pm\alpha_S z} \right\} \mathrm{e}^{\mathrm{i}(\beta x + \gamma y)} \tag{16}$$

$$\sigma_{XY}^{(1,2)} = 2\mu \left\{ A^{(1,2)} \beta\gamma \mathrm{e}^{\pm\alpha_L z} \pm \frac{\mathrm{i}}{\alpha_S} \left[B_1^{(1,2)} \left(\gamma^2\beta + \beta\alpha_S^2 - \beta^3\right) + B_2^{(1,2)} \left(\gamma^3 - \gamma\alpha_S^2 - \beta^2\gamma\right) \right] \mathrm{e}^{\pm\alpha_S z} \right\} \mathrm{e}^{\mathrm{i}(\beta x + \gamma y)} \tag{17}$$

$$\sigma_{XZ}^{(1,2)} = 2\mu \left\{ \mp \mathrm{i} A^{(1,2)} \beta\alpha_L \mathrm{e}^{\pm\alpha_L z} + \left[2B_1^{(1,2)} \beta\gamma + B_2^{(1,2)} \left(\gamma^2 - \alpha_S^2 - \beta^2\right) \right] \mathrm{e}^{\pm\alpha_S z} \right\} \mathrm{e}^{\mathrm{i}(\beta x + \gamma y)} \tag{18}$$

$$\sigma_{YY}^{(1,2)} = \mu \left\{ A^{(1,2)} \left(\gamma^2 - \beta^2 - \alpha_S^2 + 2\alpha_L^2\right) \mathrm{e}^{\pm\alpha_L z} \pm \frac{4\mathrm{i}\gamma}{\alpha_S} \left[B_1^{(1,2)} \left(\alpha_S^2 - \beta^2\right) - B_2^{(1,2)} \beta\gamma \right] \mathrm{e}^{\pm\alpha_S z} \right\} \mathrm{e}^{\mathrm{i}(\beta x + \gamma y)} \tag{19}$$

$$\sigma_{YZ}^{(1,2)} = 2\mu \left\{ \mp \mathrm{i} A^{(1,2)} \gamma\alpha_L \mathrm{e}^{\pm\alpha_L z} + \left[B_1^{(1,2)} \left(\alpha_S^2 + \gamma^2 - \beta^2\right) - 2B_2^{(1,2)} \beta\gamma \right] \mathrm{e}^{\pm\alpha_S z} \right\} \mathrm{e}^{\mathrm{i}(\beta x + \gamma y)} \tag{20}$$

and

$$\sigma_{ZZ}^{(1,2)} = \mu \left\{ -A^{(1,2)} \left(\gamma^2 + \beta^2 + \alpha_S^2\right) \mathrm{e}^{\pm\alpha_L z} \mp 4\mathrm{i}\alpha_S \left[B_1^{(1,2)} \gamma - B_2^{(1,2)} \beta \right] \mathrm{e}^{\pm\alpha_S z} \right\} \mathrm{e}^{\mathrm{i}(\beta x + \gamma y)}. \tag{21}$$

These are general solutions for the displacement and stress components, expressed in terms of arbitrary functions $A^{(m)}$ and $B_n^{(m)}$ $(m = 1,2; n = 1,2,3)$, which depend on the boundary conditions of a given problem.

BOUNDARY CONDITIONS

In order to obtain the expressions of $A^{(m)}$ and $B_n^{(m)}$ for the title problem (a full-space), equilibrium and kinematic compatibility conditions are imposed for $m = 1$ and $m = 2$ parts of the full-space. The kinematic compatibility condition for this problem can be written as

$$u_j^{(1)}(x, y, z = 0) = u_j^{(2)}(x, y, z = 0), \tag{22}$$

and the equilibrium condition can be expressed as

$$\sigma_{Zj}^{(1)}(x, y, z = 0) - \sigma_{Zj}^{(2)}(x, y, z = 0) = p_j(x, y). \tag{23}$$

The discontinuity p_j in the expression of σ_{Zj} in the $x-y$ plane $(z = 0)$ is the external load applied at the interface between media $m = 1$ and $m = 2$ (Fig. 1), which has magnitude $\bar{p}_j$ and is applied in the $j-$direction $(j = x, y, z)$. Assuming time-harmonic loads, p_j is given by

$$p_j(x, y) = \bar{p}_j(x, y) \mathrm{e}^{\mathrm{i}(\beta x + \gamma y)}. \tag{24}$$

Equations 22 and 23 involve six algebraic equations, the solution of which yields

$$A^{(1,2)} = \frac{1}{2}\mathrm{i}\frac{\beta\bar{p}_X(\beta,\gamma)}{\alpha_L\mu k_S^2} + \frac{1}{2}\frac{\gamma\bar{p}_Y(\beta,\gamma)}{\alpha_L\mu k_S^2} \pm \frac{1}{2}\frac{\bar{p}_Z(\beta,\gamma)}{\mu k_S^2}, \tag{25}$$

$$B_1^{(1,2)} = \mp\frac{1}{4}\frac{\bar{p}_Y(\beta,\gamma)}{\mu k_S^2} + \frac{1}{4}\frac{\gamma\bar{p}_Z(\beta,\gamma)}{\alpha_S\mu k_S^2}, \tag{26}$$

$$B_2^{(1,2)} = \pm\frac{1}{4}\frac{\bar{p}_X(\beta,\gamma)}{\mu k_S^2} - \frac{1}{4}\mathrm{i}\frac{\beta\bar{p}_Z(\beta,\gamma)}{\alpha_S\mu k_S^2}. \tag{27}$$

Biquadratic external loads

In this paper, the magnitude $\bar{p}_j$ of the external load is assumed to have a biquadratic variation over the square patch $|x|<A; |y|<B; z=0$ of the full-space (Fig. 1). An expression for this distribution can be established by direct interpolation of its value at specific points. Consider the points $Q_1=(+A,+B,0)$, $Q_2=(+A,0,0)$, $Q_3=(+A,-B,0)$, $Q_4=(0,-B,0)$, $Q_5=(-A,-B,0)$, $Q_6=(-A,0,0)$, $Q_7=(-A,+B,0)$, $Q_8=(0,+B,0)$, $Q_9=(0,0,0)$. The value of $\bar{p}_j$ at Q_i is denoted as t_i $(i=1,...,9)$. An expression for $\bar{p}_j$ can be obtained by a biquadratic interpolation over $\bar{p}_j(Q_i)=t_i$ as

$$\bar{p}_j(x,y,z=0)=\frac{1}{4A^2B^2}\left(T_1x^2y^2+T_2Bx^2y+2T_3B^2x^2+T_4ABxy+T_5Axy^2+2T_6AB^2x+2T_7A^2y^2\ +2T_8A^2By+4T_9A^2B^2\right), \tag{28}$$

for $|x|<A$ and $|y|<B$, and $\bar{p}_j(x,y,z=0)=0$ otherwise, in which

$$T_1=t_1+t_3+t_5+t_7+4t_9-2(t_2+t_4+t_6+t_8), \tag{29}$$

$$T_2=t_1+2t_4+t_7-(t_3+t_5+2t_8), \tag{30}$$

$$T_3=t_2+t_6-2t_9, \tag{31}$$

$$T_4=t_1+t_5-(t_3+t_7), \tag{32}$$

$$T_5=t_1+t_3+2t_6-(2t_2+t_5+t_7), \tag{33}$$

$$T_6=t_2-t_6, T_7=t_4+t_8-2t_9, \tag{34}$$

$$T_8=-t_4+t_8, \tag{35}$$

and

$$T_9=t_9. \tag{36}$$

Since Equation 23 is written in the (β,γ) domain, Eq. 28 must undergo a Fourier transform so that it can be incorporated into that equation. This transformation yields

$$\bar{p}_j(\beta,\gamma)=-\frac{1}{2A^2B^2\pi\beta^3\gamma^3}\sum_{i=1}^{9}\bar{p}_{ij}, \tag{37}$$

in which

$$\frac{\bar{p}_{1j}}{T_1}=\left(\beta^2A^2-2\right)\left(\gamma^2B^2-2\right)\sin(\beta A)\sin(\gamma B)+2B\gamma\left(\beta^2A^2-2\right)\sin(\beta A)\cos(\gamma B) \\ +2\beta A\left(\gamma^2B^2-2\right)\cos(\beta A)\sin(\gamma B)+4AB\beta\gamma\cos(\beta A)\cos(\gamma B), \tag{38}$$

$$\frac{\bar{p}_{2j}}{T_2 i\gamma B}=-\left(\beta^2A^2-2\right)\sin(\beta A)\sin(\gamma B)+B\gamma\left(\beta^2A^2-2\right)\sin(\beta A)\cos(\gamma B) \\ -2\beta A\cos(\beta A)\sin(\gamma B)+2AB\beta\gamma\cos(\beta A)\cos(\gamma B), \tag{39}$$

$$\frac{\bar{p}_{3j}}{2T_3\beta^2\gamma^2}=\left(\beta^2A^2-2\right)\sin(\beta A)\sin(\gamma B)+2A\beta\cos(\beta A)\sin(\gamma B), \tag{40}$$

$$\frac{\bar{p}_{4j}}{T_4AB\beta\gamma}=-\sin(\beta A)\sin(\gamma B)+\gamma B\sin(\beta A)\cos(\gamma B)+A\beta\cos(\beta A)\sin(\gamma B)-AB\beta\gamma\cos(\beta A)\cos(\gamma B), \tag{41}$$

$$\frac{\bar{p}_{5j}}{T_5 iA\beta}=-\left(\gamma^2B^2-2\right)\sin(\beta A)\sin(\gamma B)-2B\gamma\sin(\beta A)\cos(\gamma B) \\ +A\beta\left(\gamma^2B^2-2\right)\cos(\beta A)\sin(\gamma B)+2AB\beta\gamma\cos(\beta A)\cos(\gamma B), \tag{42}$$

$$\frac{\bar{p}_{6j}}{2T_6 \mathrm{i} A B^2 \beta \gamma^2} = -B\gamma \sin(\beta A)\sin(\gamma B) + AB\beta\gamma \cos(\beta A)\sin(\gamma B), \tag{43}$$

$$\frac{\bar{p}_{7j}}{2T_7 A^2 \beta^2} = \left(\gamma^2 B^2 - 2\right)\sin(\beta A)\sin(\gamma B) + 2B\gamma \sin(\beta A)\cos(\gamma B), \tag{44}$$

$$\frac{\bar{p}_{8j}}{2T_8 \mathrm{i} A^2 B \beta^2 \gamma} = -\sin(\beta A)\sin(\gamma B) + B\gamma \sin(\beta A)\cos(\gamma B), \tag{45}$$

and

$$\frac{\bar{p}_{9j}}{4T_9 A^2 B^2 \beta^2 \gamma^2} = \sin(\beta A)\sin(\gamma B). \tag{46}$$

DISPLACEMENT FIELDS

The final step in the derivation consists in substituting the expressions for $A^{(m)}$ and $B_n^{(m)}$ for the full-space case (Eqs. Eqs. 25 to 27) into the general expressions of displacement components u_i (Eqs. 13 to 15), considering the expression for the external load in the (β, γ) domain (Eq. 37). This results in the final expressions of the displacement field in the (β, γ) domain. Their counterparts in the physical domain are obtained after subjecting these expressions to direct Fourier transform, which yields:

$$\begin{aligned}
\frac{u_{XZ}}{D_N}\frac{z}{|z|} &= -T_1\frac{A^3}{a_0^3}\int_0^\infty\left(\int_0^\infty F_1\frac{F_{\beta 1}}{k_\beta^2}s_{\beta x}dk_\beta\right)\frac{F_{\gamma 1}}{k_\gamma^3}c_{\gamma y}dk_\gamma \\
&+ T_2\frac{A^2B}{a_0^2}\int_0^\infty\left(\int_0^\infty F_1\frac{F_{\beta 1}}{k_\beta^2}s_{\beta x}dk_\beta\right)\frac{F_{\gamma 2}}{k_\gamma^2}s_{\gamma y}dk_\gamma - T_3\frac{2AB^2}{a_0}\int_0^\infty\left(\int_0^\infty F_1\frac{F_{\beta 1}}{k_\beta^2}s_{\beta x}dk_\beta\right)\frac{s_{\gamma B}}{k_\gamma}c_{\gamma y}dk_\gamma \\
&+ T_4\frac{A^2B}{a_0}\int_0^\infty\left(\int_0^\infty F_1\frac{F_{\beta 2}}{k_\beta}c_{\beta x}dk_\beta\right)\frac{F_{\gamma 2}}{k_\gamma^2}s_{\gamma y}dk_\gamma - T_5\frac{A^3}{a_0^2}\int_0^\infty\left(\int_0^\infty F_1\frac{F_{\beta 2}}{k_\beta}c_{\beta x}dk_\beta\right)\frac{F_{\gamma 1}}{k_\gamma^3}c_{\gamma y}dk_\gamma \\
&- T_6 2AB^2\int_0^\infty\left(\int_0^\infty F_1\frac{F_{\beta 2}}{k_\beta}c_{\beta x}dk_\beta\right)\frac{s_{\gamma B}}{k_\gamma}c_{\gamma y}dk_\gamma - T_7\frac{2A^3}{a_0}\int_0^\infty\left(\int_0^\infty F_1 s_{\beta A}s_{\beta x}dk_\beta\right)\frac{F_{\gamma 1}}{k_\gamma^3}c_{\gamma y}dk_\gamma \\
&+ T_8 2A^2B\int_0^\infty\left(\int_0^\infty F_1 s_{\beta A}s_{\beta x}dk_\beta\right)\frac{F_{\gamma 2}}{k_\gamma^2}s_{\gamma y}dk_\gamma - T_9 4AB^2a_0\int_0^\infty\left(\int_0^\infty F_1 s_{\beta A}s_{\beta x}dk_\beta\right)\frac{s_{\gamma B}}{k_\gamma}c_{\gamma y}dk_\gamma,
\end{aligned} \tag{47}$$

$$\begin{aligned}
\frac{u_{YZ}}{D_N}\frac{z}{|z|} &= -T_1\frac{A^3}{a_0^3}\int_0^\infty\left(\int_0^\infty F_1\frac{F_{\beta 1}}{k_\beta^3}c_{\beta x}dk_\beta\right)\frac{F_{\gamma 1}}{k_\gamma^2}s_{\gamma y}dk_\gamma \\
&- T_2\frac{A^2B}{a_0^2}\int_0^\infty\left(\int_0^\infty F_1\frac{F_{\beta 1}}{k_\beta^3}c_{\beta x}dk_\beta\right)\frac{F_{\gamma 2}}{k_\gamma}c_{\gamma y}dk_\gamma - T_3\frac{2AB^2}{a_0}\int_0^\infty\left(\int_0^\infty F_1\frac{F_{\beta 1}}{k_\beta^3}c_{\beta x}dk_\beta\right)s_{\gamma B}s_{\gamma y}dk_\gamma \\
&+ T_4\frac{A^2B}{a_0}\int_0^\infty\left(\int_0^\infty F_1\frac{F_{\beta 2}}{k_\beta^2}s_{\beta x}dk_\beta\right)\frac{F_{\gamma 2}}{k_\gamma}c_{\gamma y}dk_\gamma + T_5\frac{A^3}{a_0^2}\int_0^\infty\left(\int_0^\infty F_1\frac{F_{\beta 2}}{k_\beta^2}s_{\beta x}dk_\beta\right)\frac{F_{\gamma 1}}{k_\gamma^2}s_{\gamma y}dk_\gamma \\
&+ T_6 2AB^2\int_0^\infty\left(\int_0^\infty F_1\frac{F_{\beta 2}}{k_\beta^2}s_{\beta x}dk_\beta\right)s_{\gamma B}s_{\gamma y}dk_\gamma - T_7\frac{2A^3}{a_0}\int_0^\infty\left(\int_0^\infty F_1\frac{s_{\beta A}}{k_\beta}c_{\beta x}dk_\beta\right)\frac{F_{\gamma 1}}{k_\gamma^2}s_{\gamma y}dk_\gamma \\
&- T_8 2A^2B\int_0^\infty\left(\int_0^\infty F_1\frac{s_{\beta A}}{k_\beta}c_{\beta x}dk_\beta\right)\frac{F_{\gamma 2}}{k_\gamma}c_{\gamma y}dk_\gamma - T_9 4AB^2a_0\int_0^\infty\left(\int_0^\infty F_1\frac{s_{\beta A}}{k_\beta}c_{\beta x}dk_\beta\right)s_{\gamma B}s_{\gamma y}dk_\gamma,
\end{aligned} \tag{48}$$

and

$$\frac{u_{ZZ}}{D_N} = -T_1\frac{A^3}{a_0^3}\int_0^\infty\left(\int_0^\infty \frac{F_2}{\bar{\alpha}_S}\frac{F_{\beta 1}}{k_\beta^3}c_{\beta x}dk_\beta\right)\frac{F_{\gamma 1}}{k_\gamma^3}c_{\gamma y}dk_\gamma$$
$$+T_2\frac{A^2B}{a_0^2}\int_0^\infty\left(\int_0^\infty \frac{F_2}{\bar{\alpha}_S}\frac{F_{\beta 1}}{k_\beta^3}c_{\beta x}dk_\beta\right)\frac{F_{\gamma 2}}{k_\gamma^2}s_{\gamma y}dk_\gamma - T_3\frac{2AB^2}{a_0}\int_0^\infty\left(\int_0^\infty \frac{F_2}{\bar{\alpha}_S}\frac{F_{\beta 1}}{k_\beta^3}c_{\beta x}dk_\beta\right)\frac{s_{\gamma B}}{k_\gamma}c_{\gamma y}dk_\gamma$$
$$-T_4\frac{A^2B}{a_0}\int_0^\infty\left(\int_0^\infty \frac{F_2}{\bar{\alpha}_S}\frac{F_{\beta 2}}{k_\beta^2}s_{\beta x}dk_\beta\right)\frac{F_{\gamma 2}}{k_\gamma^2}s_{\gamma y}dk_\gamma + T_5\frac{A^3}{a_0^2}\int_0^\infty\left(\int_0^\infty \frac{F_2}{\bar{\alpha}_S}\frac{F_{\beta 2}}{k_\beta^2}s_{\beta x}dk_\beta\right)\frac{F_{\gamma 1}}{k_\gamma^3}c_{\gamma y}dk_\gamma$$
$$+T_6 2AB^2\int_0^\infty\left(\int_0^\infty \frac{F_2}{\bar{\alpha}_S}\frac{F_{\beta 2}}{k_\beta^2}s_{\beta x}dk_\beta\right)\frac{s_{\gamma B}}{k_\gamma}c_{\gamma y}dk_\gamma - T_7\frac{2A^3}{a_0}\int_0^\infty\left(\int_0^\infty \frac{F_2}{\bar{\alpha}_S}\frac{s_{\beta A}}{k_\beta}c_{\beta x}dk_\beta\right)\frac{F_{\gamma 1}}{k_\gamma^3}c_{\gamma y}dk_\gamma$$
$$+T_8 2A^2B\int_0^\infty\left(\int_0^\infty \frac{F_2}{\bar{\alpha}_S}\frac{s_{\beta A}}{k_\beta}c_{\beta x}dk_\beta\right)\frac{F_{\gamma 2}}{k_\gamma^2}s_{\gamma y}dk_\gamma - T_9 4AB^2a_0\int_0^\infty\left(\int_0^\infty \frac{F_2}{\bar{\alpha}_S}\frac{s_{\beta A}}{k_\beta}c_{\beta x}dk_\beta\right)\frac{s_{\gamma B}}{k_\gamma}c_{\gamma y}dk_\gamma, \quad (49)$$

in which

$$k_\beta = \frac{A}{a_0}\beta, k_\gamma = \frac{A}{a_0}\gamma, \quad (50)$$

$$D_N = -\frac{\eta_r + i\eta_i}{2\mu\pi^2B^2a_0^2}, \quad (51)$$

$$s_{\beta x} = \sin\left(\frac{a_0}{A}k_\beta x\right), s_{\gamma y} = \sin\left(\frac{a_0}{A}k_\gamma y\right), s_{\beta A} = \sin\left(a_0k_\beta\right), s_{\gamma B} = \sin\left(a_0b_0k_\gamma\right), \quad (52)$$

$$c_{\beta x} = \cos\left(\frac{a_0}{A}k_\beta x\right), c_{\gamma y} = \cos\left(\frac{a_0}{A}k_\gamma y\right), c_{\beta A} = \cos\left(a_0k_\beta\right), c_{\gamma B} = \cos\left(a_0b_0k_\gamma\right), \quad (53)$$

$$b_0 = \frac{B}{A}, a_0 = A\omega\sqrt{\frac{\rho}{\mu}}, \quad (54)$$

$$\bar{\alpha}_L^2 = \left(k_\beta^2 + k_\gamma^2\right) - \frac{\left(k_L^*/k_S^*\right)^2}{\eta_r + i\eta_i}, \bar{\alpha}_S^2 = \left(k_\beta^2 + k_\gamma^2\right) - \frac{1}{\eta_r + i\eta_i}, \quad (55)$$

$$F_1 = e^{-\frac{a_0}{A}\bar{\alpha}_L|z|} - e^{-\frac{a_0}{A}\bar{\alpha}_S|z|}, F_2 = \bar{\alpha}_L\bar{\alpha}_S e^{-\frac{a_0}{A}\bar{\alpha}_L|z|} - \left(k_\beta^2 + k_\gamma^2\right)e^{-\frac{a_0}{A}\bar{\alpha}_S|z|}, \quad (56)$$

$$F_{\beta 1} = \left(a_0^2k_\beta^2 - 2\right)s_{\beta A} + 2a_0k_\beta c_{\beta A}, F_{\beta 2} = -s_{\beta A} + a_0k_\beta c_{\beta A}, \quad (57)$$

$$F_{\gamma 1} = \left(b_0^2a_0^2k_\gamma^2 - 2\right)s_{\gamma B} + 2b_0a_0k_\gamma c_{\gamma B}, F_{\gamma 2} = -s_{\gamma B} + b_0a_0k_\gamma c_{\gamma B}. \quad (58)$$

NUMERICAL RESULTS

Analytical solutions for Eqs. 47 to 49 are possibly unattainable. Their numerical evaluation requires carefully selected methods. The integrands are characterized by the existence of two distinct regions. For small values of k_β and k_γ, the integrand contains two singularities, corresponding to the primary and secondary wave numbers in the full-space. In soil problems, these are physically related to the compression (P) and shear (S) wave numbers, respectively. In the present implementation, the integral in this region is evaluated via the combination of two techniques. The first is the incorporation of a small damping factor $\eta = 0.001$ into the constitutive parameters according to Christensen's elastic-viscoelastic correspondence principle (Christensen, 2010). According to this principle, new complex values for the constitutive parameters of the full-space are obtained as $\lambda^* = \lambda(1+i\eta)$ and $\mu^* = \mu(1+i\eta)$, which are used instead of μ and λ in Eq. 1. This has little consequence to the model of the soil for engineering practice, but it smooths out the singularities and facilitates the evaluation of their integrals (Michalski and Mosig, 2016). The smoothed singular region is then integrated via classical adaptive Gaussian quadrature routines (Piessens et al., 2012). For larger values of k_β and k_γ, the integrands of Eqs. 47 to 49 present an oscillatory-decaying behavior, the integral of which only converges at infinity. It has been found that extrapolation-based techniques involving improved versions of the Longman's method (Longman, 1956) are capable of

evaluating the integral of these regions accurately. A detailed description of the methods used to evaluate these integrals can be found in Labaki et al. (2012).

The present implementation has been extensively validated by comparing its results with those of limiting cases from the literature, such as Kelvin's point load problem (Kane, 1994), the 2D plane-strain problem solved by Barros and Mesquita (1999), and the dynamic point-load Kelvin solution (Kitahara, 2014). The case of biquadratically-varying loads, which has not been solved in the literature, has been validated by checking whether stress solutions reproduce the boundary conditions for measuring points near the loaded area, and by comparing stress solutions that have been synthesized numerically from displacement solutions with those that have been computed directly. A scheme for the numerical synthetization of stress components from displacement components is presented by Romanini et al. (2021). The comparisons showed that the present implementation is capable of reproducing previous results accurately, and that it yields physically-consistent displacement responses.

All results in this section consider $\mu = 1$, $\rho = 1$, $\nu = 0.25$, and $A = B = 1$.

Figures 2 and 3 show displacement fields due to various load distributions. Loading cases A, B, and C consider $t_i = 1/(4AB)$ $(i = 1:9)$ (constant load distribution), $t_i = 3i/(80AB)$, and $t_{1:8} = 0; t_9 = 9/(16AB)$. The magnitude of these loads is such that they have unit net values: $\int_{-A}^{A}\int_{-B}^{B} \bar{p}(x,y)\,dxdy = 1$. This definition is planned in order to highlight the effect of loading distribution, rather than magnitude, in the response of the full-space. All cases consider the frequency of excitation $a_0 = 1$.

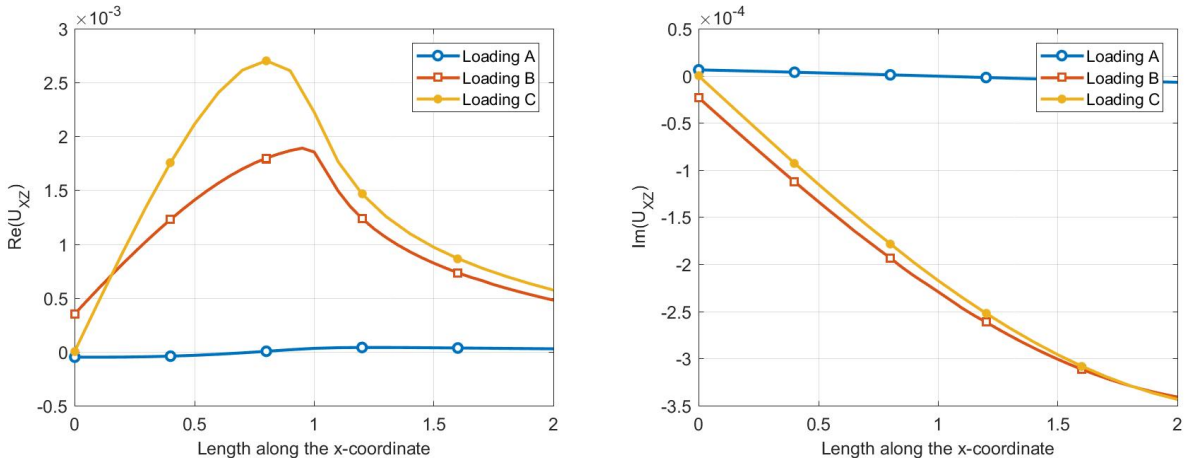

Figure 2 – Effect of different load distributions on u_{XZ}.

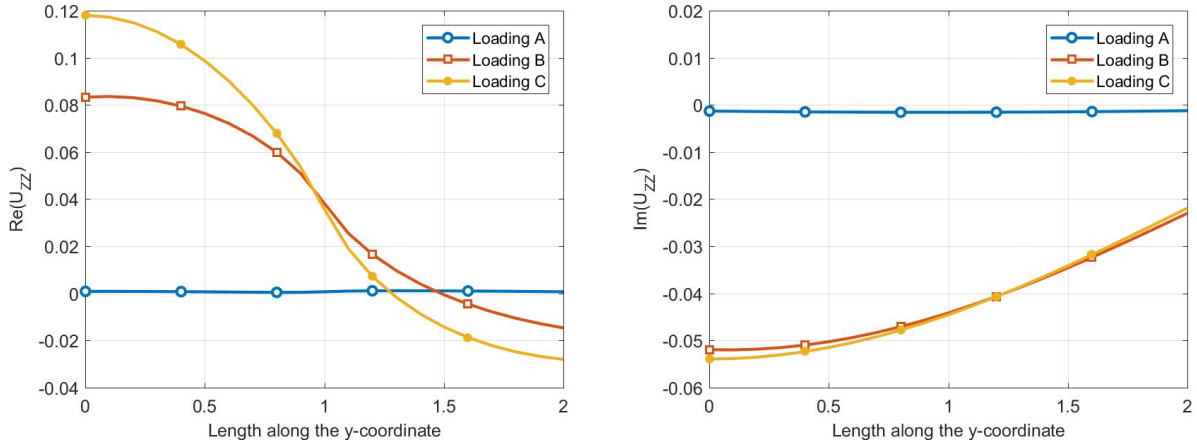

Figure 3 – Effect of different load distributions on u_{ZZ}.

Figures 2 and 3 show that displacement fields are strongly dependent on the distribution of the load. Loads that are

not uniformly distributed present more abrupt variations along the measured like than the uniformly-distributed loading case A. These effects are more pronounced near the loaded area ($x, y < A$), as expected. It is physically consistent that the overall magnitude of the direct displacement component u_{ZZ} is larger than the magnitude of the cross displacement component u_{XZ}, which is observed for all loading distributions.

CONCLUSIONS

This paper presented a novel solution for the displacement response of three-dimensional full-spaces under time-harmonic vertical loads. The derivation consisted in obtained expressions for the coupled equations of motion and the external load in the Fourier domain, in which boundary conditions corresponding to the full-space problem were able to be imposed algebraically. These solutions correspond to non-singular influence functions, which can be used in the framework of boundary element and meshless methods to solve elastodynamic problems. The consideration of biquadratic variation of the external loads makes these functions more suitable to represent sharp contact traction variations, which are common in engineering practice.

ACKNOWLEDGMENTS

The research leading to this article has been funded by the São Paulo Research Foundation (Fapesp) through grant 2013/08293-7 (CEPID). The support of PROPP/UFMS is also gratefully acknowledged.

REFERENCES

Adolph, M., Mesquita, E., Carvalho, E. R., and Romanini, E., 2007. "Numerically evaluated displacement and stress solutions for a 3D viscoelastic half space subjected to a vertical distributed surface stress loading using the radon and Fourier transforms". Communications in Numerical Methods in Engineering, 23(8):787–804.

Ba, Z., Liang, J., Lee, V. W., and Hu, L., 2018a. "IBEM for impedance functions of an embedded strip foundation in a multi-layered transversely isotropic half-space". Journal of Earthquake Engineering, 22(8):1415–1446.

Ba, Z., Liang, J., Lee, V. W., and Kang, Z., 2018b. "Dynamic impedance functions for a rigid strip footing resting on a multi-layered transversely isotropic saturated half-space". Engineering Analysis with Boundary Elements, 86:31–44.

Ba, Z., Wang, Y., Liang, J., and Lee, V. W., 2020. "Wave scattering of plane P, SV, and SH waves by a 3D alluvial basin in a multilayered half-space". Bulletin of the Seismological Society of America, 110(2):576–595.

Barros, P. and Mesquita, E., 1999. "Elastodynamic greens functions for orthotropic planestrain continua with inclined axes of symmetry". International Journal of Solids and Structures, 36(31-32):4767–4788.

Barros, P. and Mesquita, E., 2000. "Singular-ended spline interpolation for two-dimensional boundary element analysis". International Journal for Numerical Methods in Engineering, 47(5):951–967.

Barros, P. and Mesquita, E., 2009. "The response of an elastic half-space with circular trenches around a rigid surface foundation subjected to dynamic horizontal loads". Proceedings of the 10th International Conference on Boundary Element Techniques.

Carneiro, D., Barros, P. L. A. and Labaki, J., 2022. "Ground vibration attenuation performance of surface walls". Computers and Geotechnics, 1:28.

Christensen, R. M., 2010. "Theory of Viscoelasticity: Second Edition" (Dover Civil and Mechanical Engineering). Dover Publications.

Dumont, N. A., 1994. "On the efficient numerical evaluation of integrals with complex singularity poles". Engineering Analysis with Boundary Elements, 13(2):155–168.

Fu, J., Liang, J., and Ba, Z., 2019. "Non-singular boundary element method on impedances of three-dimensional rectangular foundations". Engineering Analysis with Boundary Elements, 99:100–110.

Fu, J., Liang, J., and Han, B., 2017. "Impedance functions of three-dimensional rectangular foundations embedded in multi-layered half-space". Soil Dynamics and Earthquake Engineering, 103:118–122.

Guerra, C., Labaki, J., and Barros, P. L. A., 2022. "Dynamic response of large diameter, concrete-lined vertical shafts under external and seismic excitation". International Journal for Numerical and Analytical Methods in Geomechanics, 1:28.

Helmholtz, H., 1858. "About integrals of hydrodynamic equations related with vortical motions". J. für die Reine Angewandte Mathematik, 55:25.

Kane, J. H., 1994. "Boundary element analysis in engineering continuum mechanics". Englewood Cliffs, NJ: Prentice Hall, 1994.

Kitahara, M., 2014. "Boundary integral equation methods in eigenvalue problems of elastodynamics and thin plates". Elsevier.

Kuzuoglu, M. and Mittra, R., 1997. "Investigation of nonplanar perfectly matched absorbers for finite element mesh truncation". IEEE Transactions on Antennas and Propagation, 45(3):474–486.

Labaki, J., Adolph, M., and Mesquita, E., 2019. "A derivation of nonsingular displacement and stress fields within a 3D full-space through Radon transforms". Engineering Analysis with Boundary Elements, 106:624–633.

Labaki, J., Romanini, E., and Mesquita, E., 2012. "Stationary dynamic displacement solutions for a rectangular load applied within a 3D viscoelastic isotropic full space - Part II: Implementation, validation, and numerical results". Mathematical Problems in Engineering, 2012.

Longman, I. M., 1956. "Note on a method for computing infinite integrals of oscillatory functions". Mathematical Proceedings of the Cambridge Philosophical Society, Vol. 52, No. 4, pp. 764-768.

Mesquita, E., Adolph, M., Barros, P., and Romanini, E., 2003. "Transient Green's functions and distributed load and solutions for plane strain, transversely isotropic and viscoelastic layers". Latin American Journal of Solids and Structures, 1(1):75–100.

Mesquita, E., Adolph, M., Carvalho, E. R., and Romanini, E., 2009a. "Dynamic displacement and stress solutions for viscoelastic half-spaces subjected to harmonic concentrated loads using the Radon and Fourier transforms". International Journal for Numerical and Analytical methods in Geomechanics, 33(18):1933–1952.

Mesquita, E., Antes, H., Thomazo, L. H., and Adolph, M., 2012a. "Transient wave propagation phenomena at viscoelastic half-spaces under distributed surface loadings". Latin American Journal of Solids and Structures, 9(4):453–474.

Mesquita, E., Labaki, J., Ferreira, L., et al., 2009b. "An implementation of the Longman's integration method on graphics hardware". CMES-Computer Modeling In Engineering & Sciences.

Mesquita, E., Romanini, E., and Labaki, J., 2012b. "Stationary dynamic displacement solutions for a rectangular load applied within a 3d viscoelastic isotropic full space – Part I: Formulation". Mathematical Problems in Engineering, 2012.

Michalski, K. A. and Mosig, J. R., 2016. "Efficient computation of Sommerfeld integral tails–methods and algorithms". Journal of Electromagnetic Waves and Applications, 30(3):281–317.

Pan, E., 2019. "Green's functions for geophysics: A review". Reports on Progress in Physics, 82(10):106801.

Piessens, R., de Doncker-Kapenga, E., Überhuber, C. W., and Kahaner, D. K., 2012. "QUADPACK: a subroutine package for automatic integration, volume 1". Springer Science & Business Media.

Romanini, E., Labaki, J., Mesquita, E., and Silva, R., 2019. "Stationary dynamic stress solutions for a rectangular load applied within a 3D viscoelastic isotropic full-space". Mathematical Problems in Engineering, 2019.

Romanini, E., Labaki, J., Vasconcelos, A., and Mesquita, E., 2021. "Influence functions for a 3D full-space under bilinear stationary loads". Engineering Analysis with Boundary Elements, 130:286–299.

Sommerfeld, A., 1949. "Partial differential equations in physics", volume 1. Academic press.

RESPONSIBILITY NOTICE

The authors are the only parties responsible for the printed material included in this paper.